

Article

Do We Need More Urban Green Space to Alleviate PM_{2.5} Pollution? A Case Study in Wuhan, China

Yuanyuan Chen ^{1,2}, Xinli Ke ^{1,*}, Min Min ¹, Yue Zhang ¹, Yaqiang Dai ¹ and Lanping Tang ^{1,3}

¹ College of Public Administration, Huazhong Agricultural University, Wuhan 430070, China; chenyan2022@webmail.hzau.edu.cn (Y.C.); mmin2010@mail.hzau.edu.cn (M.M.); yuez@webmail.hzau.edu.cn (Y.Z.); yaqiang_dai@webmail.hzau.edu.cn (Y.D.); l.p.tang@webmail.hzau.edu.cn (L.T.)

² Department of Sustainable Landscape Development, Institute for Geosciences and Geography, Martin Luther University Halle-Wittenberg, 06120 Halle (Saale), Germany

³ Department of Environmental Geography, Institute for Environmental Studies, Vrije Universiteit Amsterdam, De Boelelaan 1105, 1081 HV Amsterdam, The Netherlands

* Correspondence: kexl@mail.hzau.edu.cn

Abstract: Urban green space can help to reduce PM_{2.5} concentration by absorption and deposition processes. However, few studies have focused on the historical influence of green space on PM_{2.5} at a fine grid scale. Taking the central city of Wuhan as an example, this study has analyzed the spatiotemporal trend and the relationship between green space and PM_{2.5} in the last two decades. The results have shown that: (1) PM_{2.5} concentration reached a maximum value (139 µg/m³) in 2010 and decreased thereafter. Moran's I index values of PM_{2.5} were in a downward trend, which indicates a sparser distribution; (2) from 2000 to 2019, the total area of green space decreased by 25.83%. The reduction in larger patches, increment in land cover diversity, and less connectivity led to fragmented spatial patterns of green space; and (3) the regression results showed that large patches of green space significantly correlated with PM_{2.5} concentration. The land use/cover diversity negatively correlated with the PM_{2.5} concentration in the ordinary linear regression. In conclusion, preserving large native natural habitats can be a supplemental measure to enlarge the air purification function of the green space. For cities in the process of PM_{2.5} reduction, enhancing the landscape patterns of green space provides a win-win solution to handle air pollution and raise human well-being.

Keywords: urban green space; particulate matter; spatiotemporal evolution; landscape index; spatial panel regression



Citation: Chen, Y.; Ke, X.; Min, M.; Zhang, Y.; Dai, Y.; Tang, L. Do We Need More Urban Green Space to Alleviate PM_{2.5} Pollution? A Case Study in Wuhan, China. *Land* **2022**, *11*, 776. <https://doi.org/10.3390/land11060776>

Academic Editors: Yanan Wang, Kees Klein Goldewijk, Wei Chen, Juan Wang and Xiaosong Ren

Received: 24 April 2022

Accepted: 23 May 2022

Published: 25 May 2022

Publisher's Note: MDPI stays neutral with regard to jurisdictional claims in published maps and institutional affiliations.



Copyright: © 2022 by the authors. Licensee MDPI, Basel, Switzerland. This article is an open access article distributed under the terms and conditions of the Creative Commons Attribution (CC BY) license (<https://creativecommons.org/licenses/by/4.0/>).

1. Introduction

Urban green space can include street trees, private gardens, parks, and peri-urban agricultural land within the city [1–3]. Ecosystem benefits provided by green space significantly contribute to maintaining a livable environment for citizens. For instance, air purification [4], alleviation of urban heat islands [5,6], carbon sequestration [7], recreational service [8], and biodiversity conservation [9] can enhance the local quality of life. Small particulate matter with widths less than 2.5 µm (PM_{2.5}) is one of the outcomes of anthropogenic activities [10,11]. PM_{2.5} damages human health in terms of the cardiovascular system [12], respiration [13,14], and mortality [15]. In contrast, green spaces directly absorb particulate matter through the retention ability of leaves [16] and slow down the spread of PM_{2.5}. However, green space is often affected by urban development, which exacerbates the correlations with PM_{2.5} in areas where population density is already high.

The adverse effects of PM_{2.5} concentrations are a global concern. According to the guidelines released by the WHO, annual exposure to PM_{2.5} concentrations under 5 µg/m³ has a less negative impact on humans [17]. The guidelines and actual emissions of PM_{2.5} in many countries and regions have not yet adopted or attained the same standard yet.

For example, the two levels of PM_{2.5} concentration identified in China are 15 µg/m³ and 35 µg/m³ (annually) [18]. According to the National Ambient Air Quality Standard (NAAQS), the PM_{2.5} concentration in India should be no more than 40 µg/m³ (annually) [19]. The limit of PM_{2.5} set by the European Commission is 20 µg/m³ (annually) [20]. There are gaps between the different guidelines (Appendix A, Table A1), which indicates that many efforts need to be made in global PM_{2.5} reduction. Notably, the most dramatic influence of air pollution is the effect on longevity. Ebenstein et al. (2017) claimed that a 10.35 µg/m³ increase in PM₁₀ reduced life expectancy by 7.68 months [21]. If PM_{2.5} concentrations reach WHO air quality guidelines (annual 10 µg/m³, released in 2005) in all countries, then life expectancy will increase by a population-weighted median of 7.20 months [22]. Moreover, poor air quality exposure increases the rates of cardiovascular diseases [23,24]. In addition, regional air quality can affect citizens' self-reported happiness [25].

Governments and research institutes construct PM_{2.5} datasets to examine the concentration, possible origins, and the main influencing factors. Ground air quality stations observe hourly, daily, monthly, and yearly results of particulate matter measurements. These datasets are widely applied in spatial and temporal change analysis of PM_{2.5} [26–28] and are combined with Aerosol Optical Depths (AODs) data to generate full cover maps across regional and global scales [29,30]. PM_{2.5} concentrations and distributions are affected by anthropogenic and natural factors. The emissions from burning biomass and fossil fuels are the main origins of particulate and gaseous pollutants [31]. Landscape fires are a significant PM_{2.5} source in many regions [32]. Meteorological factors significantly influence the distribution of PM_{2.5} through wind speed and temperature [33]. Urbanization, road density, and urban morphologies correlate with PM_{2.5} pollution [34,35]. Land use and cover change also contribute to the distribution of PM_{2.5} [36]. Methods such as land-use regression, random forest, and the spatial panel model have been widely applied in examining the influencing factors and predicting the features of PM_{2.5} concentration [37–40].

Green space is one of such factors that can influence regional PM_{2.5} concentration, decreasing the concentration by deposition from leaves, affecting wind speed, and impacting air humidity [41,42]. Morphological and physiological traits of green space also make a difference in PM_{2.5} reduction [43]. Higher green space core and bridge proportions significantly reduce the PM_{2.5} concentration [44]. The leaf area index negatively correlates with PM_{2.5} mass concentration [45]. The air purification effects of green space have a particular functional scale. Considering the circular buffers of 0.5–5 km in radius, centered in the monitoring stations, the total edge length of green space has a greater impact on PM_{2.5} concentration than the green cover area. However, the influence of green cover dominates on the 3–5 km scale [46]. In addition, biogenic volatile organic compounds (BOVC) emissions of green space-induced PM_{2.5} concentration are harmful to human health [47]. The dual role of green space in warm seasons is to both remove air pollution and enhance air quality [48], which needs to be pointed out in the correlation analysis of PM_{2.5} concentration and green space morphology.

During the process of urbanization, urban green space is inevitably influenced by building encroachment. Decreasing its area will further undermine the ecosystem functions [49], especially for the central city area where impervious land occupies a higher proportion. Air purification, recreation, and habitat maintenance services of green spaces play significant roles in residents' well-being. Thus, the correlation of green space landscape patterns on PM_{2.5} concentration across an extended period needs to be clarified. Because PM_{2.5} can migrate within the regional area within a particular time, long time-series data of PM_{2.5} concentrations are more useful to develop annual full cover maps [50]. Furthermore, these maps can be fitted to examine the relationship between PM_{2.5} and green space landscape patterns on a grid scale.

This study focuses on the central city of Wuhan because it has undergone rapid urbanization and drastic changes in air quality during the last 20 years. The main objectives of the present work are to (1) reveal the spatial-temporal changes in green space and PM_{2.5} concentration and to (2) identify the correlations between landscape features of green space

and PM_{2.5} concentration. Finally, we propose strategies to enhance the positive relationship between PM_{2.5} and green space.

2. Data and Methodology

2.1. Study Area

Wuhan is the capital of Hubei province, the geographical and economic center of the middle part of China, and it has a total area of 8569.15 km² (Figure 1). It is located in a humid subtropical climate zone, and the Yangtze River flows across the central city. The annual precipitation is 2012.4 mm, and the average temperature is about 17.2 °C (2020). The total population is about 12.44 million [51], which increased by 54.67% from 2000 to 2020. Wuhan has undergone rapid urbanization over the past two decades, especially in its central districts where 57.88% of the population (7.21 million) lives.

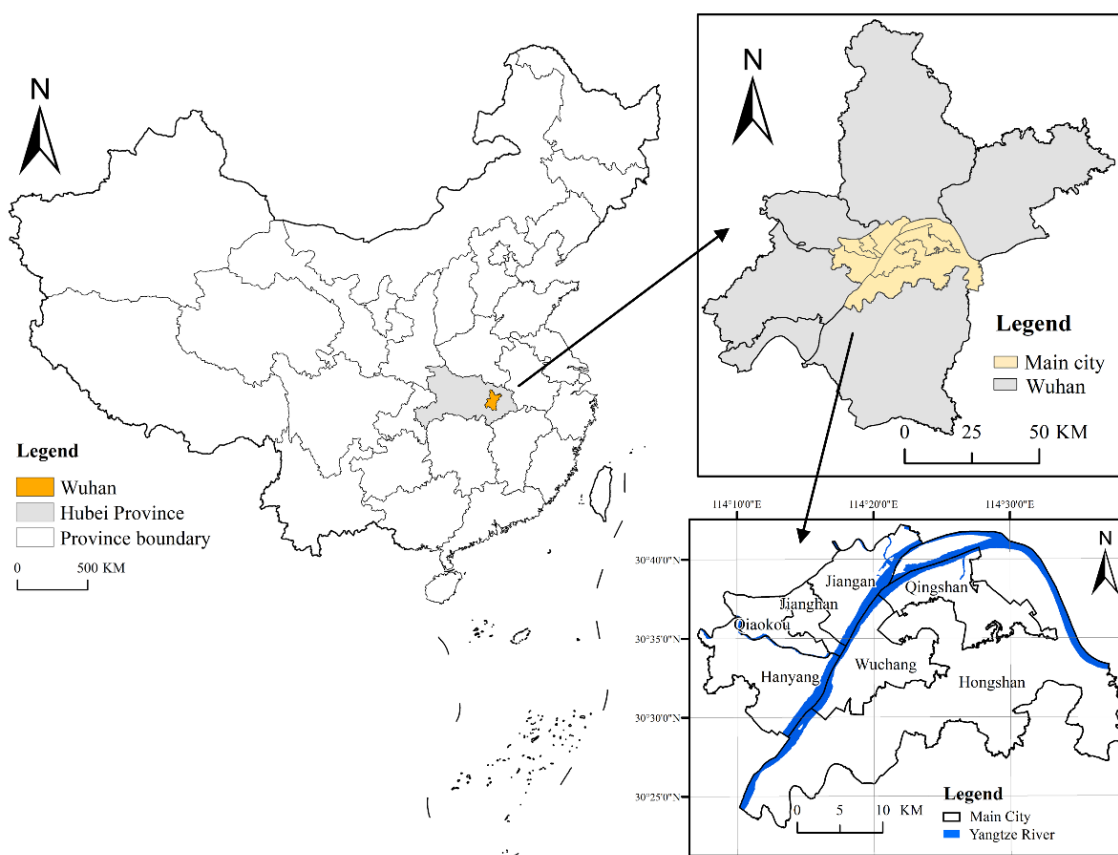


Figure 1. Location of the study area.

Expanding the impervious surface threatens the distribution pattern and amount of green space. Factory production, fossil fuel consumption, and private cars are all growing along with urban development, which causes urban problems such as air pollution and traffic jams. More attention has been given to these negative outputs and the importance of protecting the natural environment in the central districts. The local government has implemented a series of measures to deal with these problems, such as reducing energy consumption and unqualified fuels of private cars. The Chinese government gives priority status to the promotion of air quality. A PM_{2.5} concentration reduction by 10% is promised in China's 14th Five-Year Plan (2021–2025) [52], and rules such as restricting high-polluting sources and constant air quality monitoring will continue.

2.2. Data for Analysis

This study represented green space as areas composed of land cover, including woodland, grassland, and cropland. There was a rapid increase in construction land use in

the central districts, so we also considered artificial surfaces. According to the current land use classification in China (GB/T 21010-2017) [53], the land cover types were manually interpreted from Google history remote sensing images with a resolution of 2 m (2000/2010/2020) [54]. To improve the precision of our interpretation, we took the land cover maps generated from GlobalLand30 as a reference [55]. The total accuracy of GlobalLand30 is 85.72%, and the Kappa coefficient is 0.82. We calculated landscape patterns of green space in 2020. For coherence with the following data, we described the results of green space landscape patterns as in 2019.

PM_{2.5} concentration data (1 km resolution, annual average) were obtained from an open-access database [56], which includes long-term, full-coverage, and high-resolution ground-level air pollutants in China. The local government of Wuhan implemented lockdown strategies from 23 January–22 February 2020. Consequently, this study applied the PM_{2.5} dataset of 2019 in the spatial panel regression to avoid the lockdown effect. Thus, this study extracted annual PM_{2.5} concentration data from 2000, 2010, and 2019.

The spatial maps of gross domestic product (GDP) were drawn from the Data Center of Resources and Environmental Sciences (RESDC) [57]. The resolution of GDP maps in 2000, 2010, and 2015 was 1 km. Because the GDP for 2019 was unavailable, it was estimated by multiplying 2015 data by the growth rate from 2015 to 2019.

2.3. Methodology

2.3.1. Landscape Patterns of Green Space

The configuration and composition of green space can influence the deposition rate of particulate matter. Hence, we applied the total area (TA), contagion index (CONTAG), largest patch (LPI), and Shannon's diversity index (SHDI) to demonstrate the spatial distribution of green space (Table 1). TA aims to reflect the area of green space. LPI represents the dominating patches occupying the proportion of green space area. CONTAG, as the fractal dimension index, describes the spatial patterns of patches. Finally, SHDI can manifest the complexity of green space types.

Table 1. Formula and explanations of landscape indexes.

Landscape Indexes	Formula	Description	References
Total area (TA)	$TA = \sum_{j=1}^n a_{ij}$	Equals the sum of green space areas of patches.	[58,59]
Largest patch index (LPI)	$LPI = \frac{\max(a_{ij})}{A} * 100$	Equals the percentage of the landscape comprised by the giant patch	[60,61]
Contagion index (CONTAG)	$CONTAG = \left(1 + \frac{\sum_i^n \sum_j^n (P_i * m - \ln(P_i * m))}{2 \ln(n)} \right) * 100$	Ranging from 0 to 100. The lower the index value, the more scattered the urban landscape pattern and the higher the average degree of fragmentation.	[62–64]
Shannon's diversity Index (SHDI)	$SHDI = - \sum_{i=1}^n (P_i * \ln P_i)$	This represents diversity. The value increases as the number of different patch types increases.	[65,66]

Note: a_{ij} is the area (m²) of patch ij ; A is the total area of the grid (m²); n is the number of patches; P_i represents the proportion of landscape occupied by patch type i ; g_{ik} is the number of adjacencies (joins) between pixels of patch types (classes). $m = g_{ik} / \sum_{k=1}^n g_{ik}$.

A fishnet (grids with 1 km resolution) was created from the PM_{2.5} dataset (ArcGIS 10.5, "create fishnet" tool) and applied in the extraction of green space. The landscape indexes were calculated by Fragstats (4.2).

2.3.2. Spatial Correlation Analysis

(1) Spatial weight matrix

The weight matrix is based on the queen contiguity criterion to reflect the neighboring influence. Grids with the common vertexes and edges are assigned to 1, and otherwise 0. The formula is as follows:

$$W_{ij} = \begin{cases} 1, & i \text{ shares a corner or edge with } j; \\ 0, & i \text{ isn't adjacent to } j. \end{cases} \quad (1)$$

(2) Moran's I and hotspot analysis

We conducted the spatial autocorrelation test to examine the spatial interdependence of PM_{2.5} concentration. Moran's I was applied to calculate the degree of spatial autocorrelation [67,68]. The formula is expressed as follows:

$$I = \frac{\sum_{i=1}^N \sum_{j=1}^N W_{ij} (x_i - \bar{x})(x_j - \bar{x})}{s^2 \sum_{i=1}^N \sum_{j=1}^N W_{ij}} \quad (2)$$

$$s^2 = \frac{\sum_{i=1}^N (x_i - \bar{x})^2}{N} \quad (3)$$

where I is the univariate global spatial correlation index; x_i, x_j are the attribute values of features i and j , respectively; \bar{x} is the average value of features i and j ; s^2 is the sample variance; W_{ij} is the spatial weight between features i and j ; and N equals the total number of features.

For the Moran's I analysis, the null hypothesis states that the attribute being analyzed is randomly distributed among the features in the study area. The null hypothesis may be rejected when the p -value is lower than the defined threshold (5% in this study) and the z -score is positive. The spatial distribution of high values and low values in the dataset is more spatially clustered. When the p -value is lower than the defined threshold and the z -score is negative, the null hypothesis may also be rejected. In that case, the spatial distribution of high values and low values in the dataset are more spatially dispersed.

Hotspot analysis is applied to identify the clustering attribute of factors [69,70]. This analysis creates maps of statistically significant hot and cold spots. The hotspot analysis calculates the Getis-Ord G_i^* statistic for each feature in a dataset:

$$G_i^* = \frac{\sum_{j=1}^N w_{i,j} x_j - \bar{x} \sum_{j=1}^N w_{i,j}}{S \sqrt{\frac{(N \sum_{j=1}^N w_{i,j}^2 - (\sum_{j=1}^N w_{i,j})^2)}{N-1}}} \quad (4)$$

The explanations of variables are the same as in Formula (2). G_i^* is a z -score that represents the standard deviation. The resultant z -scores and p -values show where features with high or low values cluster spatially. For statistically significant positive z -scores (5% in this study), the larger z -scores represent intense clustering of high values (hot spot), and vice versa. The quadrants were divided as "High-high (H-H)", "Low-low (L-L)", "High-low (H-L)", and "Low-high (L-H)".

2.3.3. Spatial Panel Model

Variance inflation factors (VIFs) were calculated to exclude the highly correlated variables from a stepwise procedure. First, we assumed that relevant factors influenced the PM_{2.5} concentration without spatial dependency. A basic Ordinary Least Squares (OLS) model is expressed as follows:

$$Y_{it} = \beta_0 + \beta X_{it} + \varepsilon_{it} \quad (5)$$

where Y_{it} is the PM_{2.5} concentration in cell i at time t ; β_0 is a constant term; β is the parameter of X_{it} ; X_{it} represents the independent variables, referring to the landscape indexes of green space, GDP, and artificial surface proportion in this study; and ε_{it} is the error term.

Ignoring the spillover effect of PM_{2.5} concentration might lead to bias. The spatial lag model (SLM) presumes that dependent variables interact among neighbors [71,72]. Thus, we changed Formula (5) into:

$$Y_{it} = \beta_0 + \rho \sum_{j=1}^N W_{ij} Y_{it} + \beta X_{it} + \varepsilon_{it} \quad (6)$$

where ρ is the spatial lag effect coefficient. When the error terms correlate, the random effect affects the spillover effect [73]. The Spatial Error Model (SEM) is expressed as follows:

$$Y_{it} = \beta_0 + \beta X_{it} + \mu_{it} \quad (7)$$

$$\mu_{it} = \lambda W \mu_{it} + \varepsilon_{it} \quad (8)$$

where λ represents the average degree of spatial correlations of errors. Furthermore, the Spatial Durbin Model (SDM) measures the effect of neighboring dependent and independent variables [74]. In this case, PM_{2.5} concentration is influenced not only by the PM_{2.5} value of neighbors but also by the neighboring independent variables:

$$Y_{it} = \beta_0 + \rho \sum_{j=1}^N W_{ij} Y_{it} + \beta X_{it} + \theta \sum_{j=1}^N W_{ij} X_{ijt} + \varepsilon_{it} \quad (9)$$

where Y_{it} is the PM_{2.5} concentration and θ is the spatial spillover effect coefficient of the independent variables.

The Likelihood Ratio test (LR test) determines whether SLM, SEM, and SDM models are more fitted for the green space and PM_{2.5} data. The Hausman test was conducted to select between the fixed-effects (FE) or random-effects (RE) panel model [75]. Akaike's Information Criteria (AIC) and Bayesian Information Criteria (BIC) supported the model selection [76]. The lower the AIC and BIC values, the better the model fits the data. The spatial panel model was processed in Stata15 (package "xsmle").

3. Results

3.1. Temporal Change and Spatial Distribution of Green Space from 2000 to 2019

The amount of green space (TA) decreased from 381.04 km² to 282.60 km², or a decrease of 25.83%, from 2000 to 2019. Conversely, artificial surfaces increased from 290.54 km² to 387.68 km² in the same period, increasing by 33.43%. The adverse direction of transformation reflects the observation that human activities have an intervention effect on the natural environment. Consistent with the downward trend of TA, both LPI and CONTAG decreased, while SHDI increased (Table 2).

Table 2. Landscape indexes of green space in the central city from 2000 to 2019.

Year/Landscape Indexes	TA (km ²)	LPI (%)	CONTAG (%)	SHDI
2000	381.04	6.05	63.28	0.78
2010	323.52	5.93	54.81	0.96
2019	282.60	3.35	53.14	1.00
changing rate (%)				
2000–2010	−15.10	−2.04	−13.39	23.17
2010–2019	−12.65	−43.40	−3.04	4.37
2000–2019	−25.83	−44.56	−16.03	28.55

The changing rates of landscape indexes in the earlier 10 years (from 2000 to 2010) were higher than those in later years (from 2010 to 2019), except for LPI. The evolution of green space resulted in an evident reduction in total area and large patches, which led to fewer connections of natural land cover. There was an apparent downward trend in green space in the urban periphery and an incremental trend in the center area (Figure 2). In addition, landscape indexes demonstrated a clustering pattern (Appendix A, Figure A1). Moran's I for TA was in a downward trend due to the loss of ample green space around the edge of the central city. The spatial correlation of CONTAG kept increasing while LPI and SHDI decreased from 2000 to 2019. This result suggested that green space has become more fragmented and less diverse.

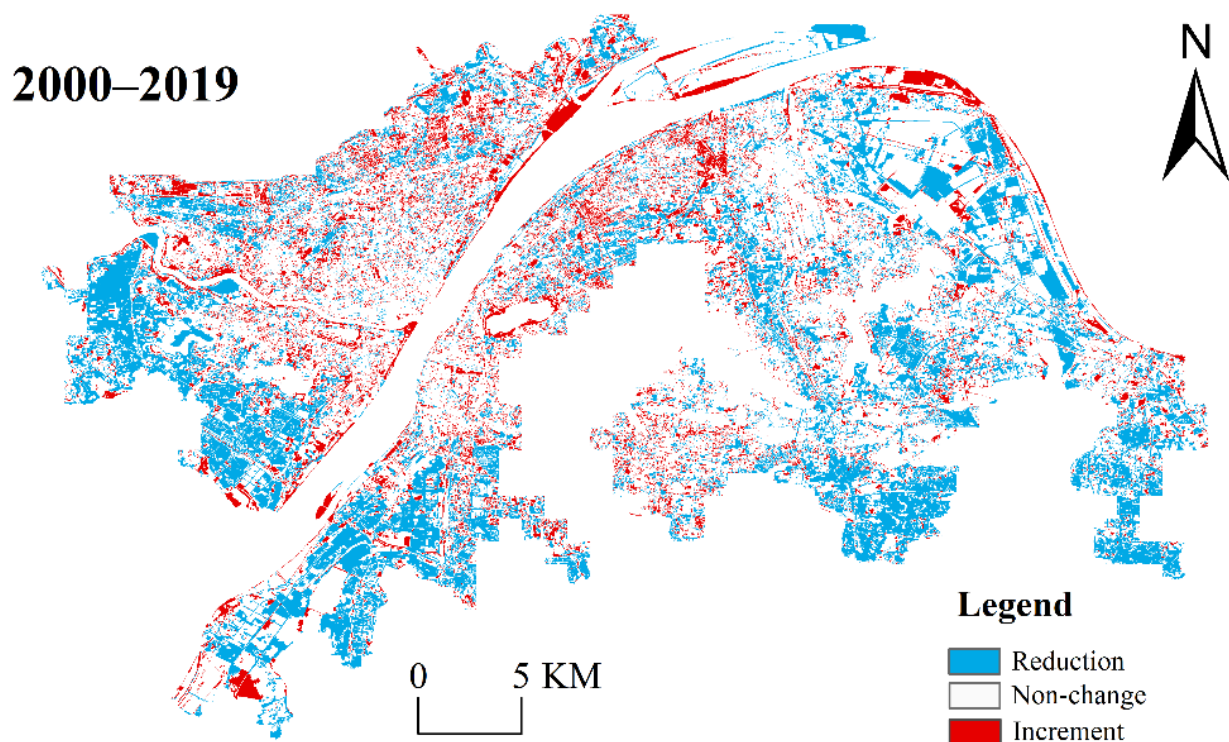


Figure 2. Spatial change in green space from 2000 to 2019 in the central city of Wuhan (reduction in blue represents the green space occupied by other types of land use; increment is the area transferred from other land use types to green space).

3.2. Spatial and Temporal Changes in $PM_{2.5}$ Concentration

From 2000 to 2019, the $PM_{2.5}$ concentration underwent a transition from an upward to a downward trend. The annual average values of $PM_{2.5}$ for 2000, 2010, and 2020 were $75.20 \mu\text{g}/\text{m}^3$, $85.87 \mu\text{g}/\text{m}^3$, and $46.10 \mu\text{g}/\text{m}^3$, respectively (Figure 3). Compared to 2000, a higher level of $PM_{2.5}$ concentration in 2010 led to an increase in the average $PM_{2.5}$ by 14.19%. The maximum value occurred in 2010. The dense $PM_{2.5}$ concentration clustered around the city center. $PM_{2.5}$ concentration decreased by 46.33% from 2010 to 2019, which corresponds with the promotion of air quality across the region. The distribution of $PM_{2.5}$ was in a clustering pattern according to the global Moran's I value from 2000 to 2019 (see Appendix A, Figure A1).

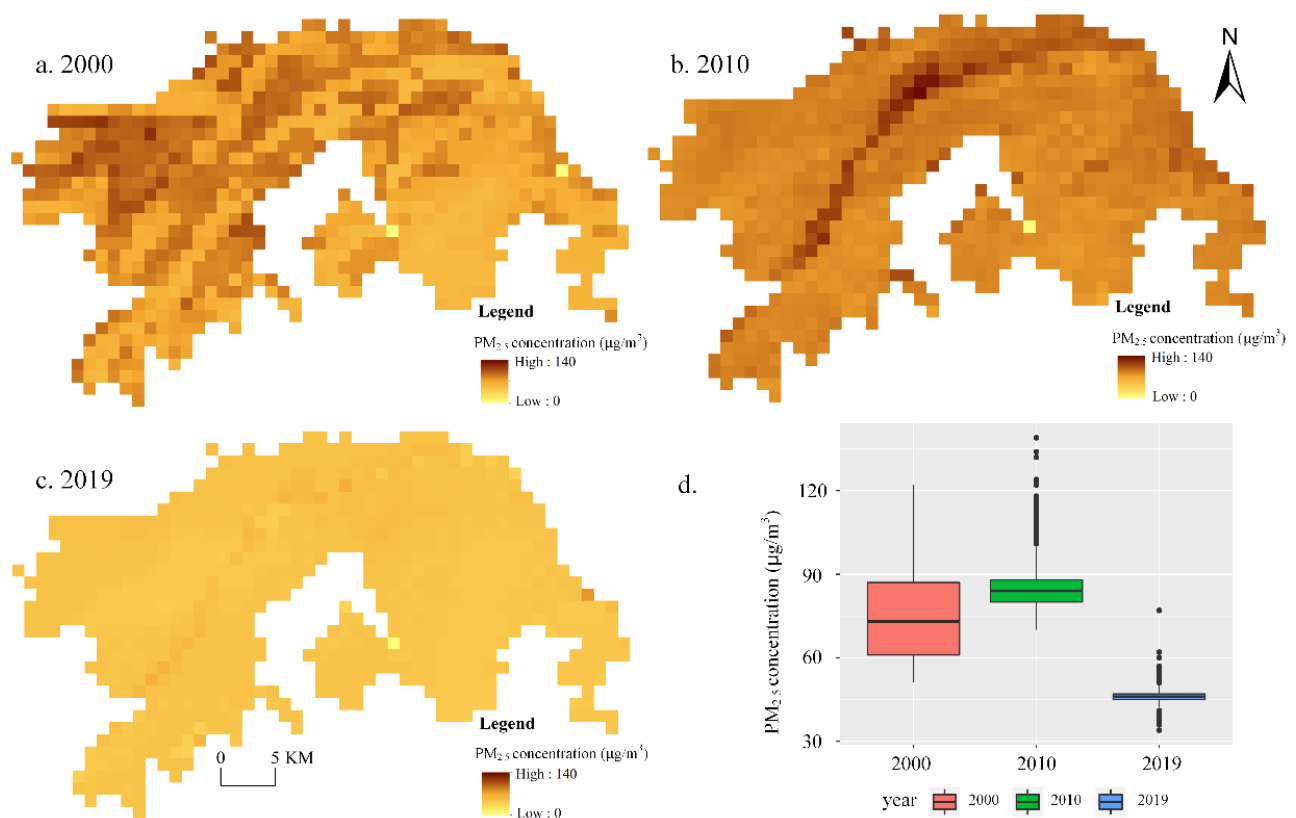


Figure 3. Spatial and temporal changes in annual $PM_{2.5}$ concentrations in the central city of Wuhan from 2000 to 2019 (a–c): $PM_{2.5}$ concentration maps were extracted from the annual $PM_{2.5}$ concentration maps of China [56]; (d): boxplot of $PM_{2.5}$ concentration. The interquartile range is from the 25th percentile to the 75th percentile. The 50th percentile is the median, represented by the middle black line).

3.3. Spatial Patterns of Green Space and $PM_{2.5}$ Concentration

The local spatial correlations among $PM_{2.5}$ concentrations and landscape indexes are shown in Figure 4. The number of grids with significant “H-H”, “H-L”, “L-H”, and “L-L” are demonstrated in the four quadrants. From 2000 to 2019, the spatial scale of “H-H” and “H-L” cluster patterns decreased, which indicates that both $PM_{2.5}$ and green space were downward. “L-L” group numbers increased on the left-hand side of the Yangtze River, while “L-H” cells clustered on the right-hand side. There were spatial correlations between $PM_{2.5}$ and green space landscape indexes. However, clarifying how the landscape patterns correlated with $PM_{2.5}$ requires further regression analysis.

3.4. Correlations of Green Space Landscape Patterns and $PM_{2.5}$ Concentration

We also considered GDP and the artificial surface area because $PM_{2.5}$ is affected by economic development and urbanization [33,34]. The VIF value of independent variables was less than 10. There was a low correlation among variables and the fit for regression analysis.

As the results have shown (Table 3), ordinary linear regression and spatial panel models examined the correlations between landscape indexes and $PM_{2.5}$ from different aspects. The R-square of OLS (0.435) showed that the landscape patterns of green space and GDP could explain the $PM_{2.5}$ concentration to a certain degree. Meanwhile, the artificial surface demonstrated an insignificant correlation with $PM_{2.5}$. GDP and $PM_{2.5}$ concentration significantly correlated. TA and LPI was negatively correlated with $PM_{2.5}$, which indicates that the area of green space and larger patches could contribute to the air purification. CONTAG demonstrated an insignificant relationship with $PM_{2.5}$ concentration. Finally, SHDI showed a strong influence in alleviating $PM_{2.5}$ concentration.

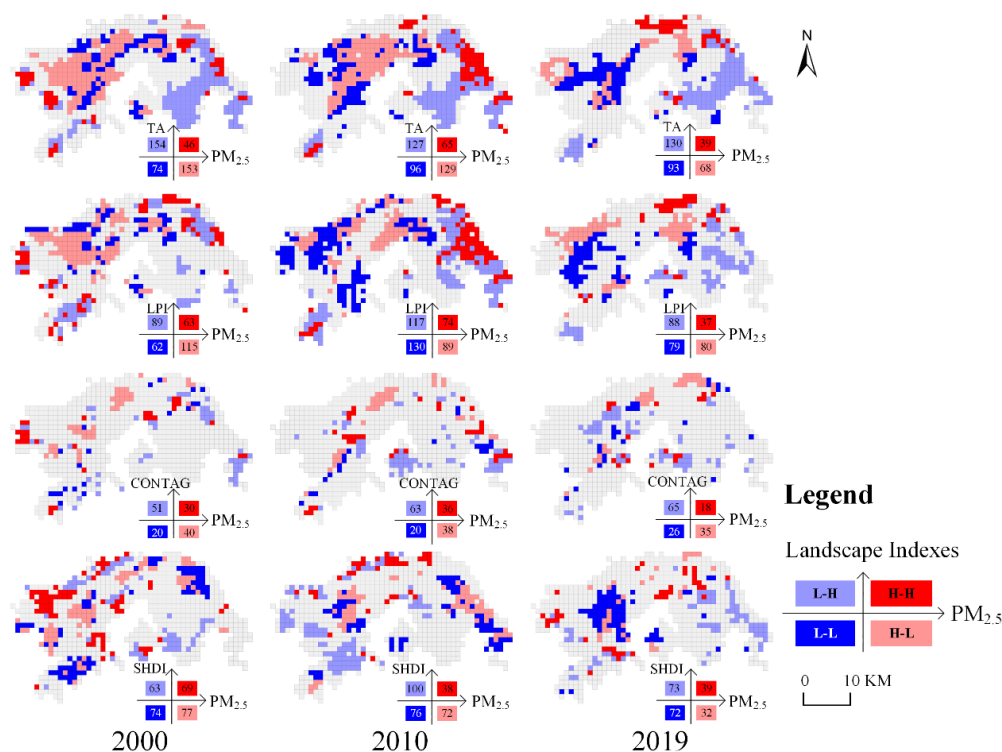


Figure 4. Local spatial correlations of PM_{2.5} and landscape patterns in the last two decades. (As mentioned in the methodology, “H-H” represents the high value of landscape indexes and PM_{2.5} concentration clusters in the spatial scale. The number inside of the rectangle is the calculation of grids, and for example, the number of “H-H” of SHDI and PM_{2.5} in 2000 is 69).

Spatial panel models further manifested the spatial correlations of PM_{2.5} and green space. LPI and GDP negatively correlated with PM_{2.5} in SLM and SEM. Neighboring GDP and TA showed a negative correlation with PM_{2.5} concentration in the results of SDM. To determine a model for further analysis, we examined the statistically significant LR and Hausman test, together with lower AIC and BIC values. We found that the spatial lag model (SLM) was more adequate. In detail, LPI negatively correlated with PM_{2.5}, which suggests the importance of protecting natural sizeable green space. Even though SHDI showed the most effective reduction in PM_{2.5}, in addition to the effect of GDP, the *p*-value was not significant. TA and CONTAG correlations with PM_{2.5} were unclear.

Table 3. Regression analysis of PM_{2.5} concentration (dependent variable) and landscape indexes, GDP, artificial surfaces.

Coefficients	Models	OLS	SLM	SEM	SDM
	Constant		169.218	-	-
Artificial surfaces		0.000	-0.009	0.002	0.006
GDP		-10.204 ***	-1.601 ***	-1.630 ***	-0.486
TA		-0.15 ***	0.006	0.032 **	0.030 **
LPI		-0.072 ***	-0.023 ***	-0.027 ***	-0.028 ***
CONTAG		-0.002	-0.007	-0.010	-0.008
SHDI		-3.64 ***	-0.597	-0.510	-0.638

Table 3. Cont.

Coefficients	Models			
	OLS	SLM	SEM	SDM
W * Artificial surfaces	-	-	-	-0.022
W * GDP	-	-	-	-1.324 ***
W * TA	-	-	-	-0.065 ***
W * LPI	-	-	-	0.026
W * CONTAG	-	-	-	0.023
W * SHDI	-	-	-	-0.197
ρ	-	0.876 ***	-	0.868 ***
λ	-	-	0.938 ***	-
Residual variance	-	30.191 ***	29.901 ***	30.145 ***
R-square	0.435	0.4254	0.2900	0.4872
AIC	20,268.721	15,859.38	15,965.58	15,853.29
BIC	20,309.385	15,905.85	16,012.05	15,934.61

Note: ***, **, * represent the significance level of p -value 1%, 5%, and 10%, respectively.

4. Discussion

This paper has focused on the relationship between green space landscape patterns and PM_{2.5} concentration in Wuhan central city over the last two decades. The significant negative correlation between LPI and PM_{2.5} was examined in the regression analysis. Reserving naturally sizeable green space and enlarging present green space are promising measures to support the mitigation of PM_{2.5}. However, impervious land constantly encroaches on surrounding green space [77]. The present study found that almost a quarter of green space vanished in the central city of Wuhan from 2000 to 2019. The loss of marginal green space exceeds the increment in the city center (Figure 2), which reduces the total area [78].

From 2010 to 2019, PM_{2.5} decreased by 46.33% in the central city of Wuhan. Policies such as the Air Pollution Prevention and the Control Action Plan, which was released by the Chinese government in 2013, significantly decreased the population-weighted annual mean PM_{2.5} concentrations in China from 61.8 to 42.0 $\mu\text{g}/\text{m}^3$ within five years [79]. Anthropogenic emission dominated the reduction. National policies could accelerate the efforts of local authorities to improve the air quality for sustainable development. In the central city of Wuhan, measures such as promoting green space coverage, reducing the use of coal, and green energy consumption have gradually alleviated regional PM_{2.5} pollution [80]. Indeed, the average PM_{2.5} concentration decreased and reached 46.1 $\mu\text{g}/\text{m}^3$ in 2019. However, this is still far from the guideline (5 $\mu\text{g}/\text{m}^3$) suggested by the WHO to reduce the harmful impacts on human health and longevity [17].

Although artificial surfaces did not show an evident relationship with PM_{2.5} concentration, the economic activities demonstrated a statistically significant correlation with PM_{2.5}. According to the Environmental Kuznets Curve, a post-urbanization period of economic development can exert a less negative influence on the environment [81,82]. In our case, during the primary period of urbanization, economic development dominated society. Factories with polluting emissions near the central city center led to poor air quality. Later, advanced economic development and urban planning would reduce the disturbance to air quality. This interpretation might explain the cluster of the “L-L” group on the left-hand side of the Yangtze River, where high urbanization and a low area of green space occur.

Notably, the relationship between green space and PM_{2.5} needs to be carefully interpreted. First, many anthropogenic and meteorological factors mutually affect PM_{2.5} concentration. The contribution rate of the main urban area source to PM_{2.5} concentration exceeds 60% in Wuhan [83]. Humidity and temperature can also contribute to the level of PM_{2.5} [84]. Even though green space features showed significant correlations with PM_{2.5} in spring [85], this mechanism is complicated. Meanwhile, biogenic volatile organic compound emissions from green space and other meteorological conditions might influence PM_{2.5} mitigation. In the context of regional climate and air quality model simulations,

vegetation emissions led to an increase in PM_{2.5} concentration over 10 µg/m³, which occupied around 20% of the average observed PM_{2.5} concentration [86]. Vegetation emissions can also increase the particle fluxes in urban environments [87]. Thus, the dual effects of vegetation need to be considered in increasing green space to achieve PM_{2.5} mitigation.

Green space landscape patterns are stressed in the present study for two reasons. First, according to previous studies, the green space area and diversification of vegetation could exert great significance in air regulation [88]. SHDI also showed a negative correlation with PM_{2.5} concentration in this study. The amount of PM_{2.5} adsorption by leaves demonstrated a noticeable seasonal difference. Conifers were more effective in PM_{2.5} adsorption than broadleaf trees were [89]. Green Infrastructure (GI) practices could significantly improve air quality in urban areas [90]. Vegetation structure, composition, and management are essential to optimize the capacity of green spaces to purify air quality [91]. The biophysical attributes of green spaces directly contribute to the reduction in PM_{2.5}. Second, the ecosystem services from green space combined with PM_{2.5} reduction could mutually affect the health of the residents [92]. Expanding the green area and reducing fragmentation can support the improvement of air quality and decrease the mortality rate of the citizens. Combined with the results of this study, large green space patches deserve more attention in urban land use planning.

This study examined the correlations between green space morphology and PM_{2.5} concentration over a long period. However, there are some limitations. First, during the lockdown period, the PM_{2.5} concentration of Wuhan decreased by 27 µg/m³ compared with the same period in 2019 [93]. In total, 90% of the reduction resulted from the lockdown because PM_{2.5} mainly comes from factories, coal consumption, and transportation. A series of research studies in India [94], America, Italy, France [95], Southern Italy [96], the United Kingdom [97], Barcelona [98], and China [99] have shown positive outcomes of promoting air quality during the same period. Although the lower pollution level briefly appeared during the lockdown, the positive effects will guide decision-makers to make more efforts to moderate PM_{2.5} concentration from the origins [100,101]. Correlations between green space and PM_{2.5} concentrations should be further investigated under different policies.

Although this study showed the possible correlations between green space morphology and PM_{2.5} concentration, the interpretation was limited by the absence of PM_{2.5} sources and meteorology data. Moreover, the physical mechanisms of green space and PM_{2.5} concentration need to be further explained. For instance, deposition on leaves might offset the emissions of biogenic volatile organic compounds, even though the net PM_{2.5} deposition of green space remains. In that case, the contribution of green space to decrease the PM_{2.5} concentration will be more comprehensive.

5. Conclusions

Urban green space landscape patterns have shown different correlations with PM_{2.5}. In the present study, LPI and SHDI negatively correlate with PM_{2.5} concentrations. Hence, it is rational to implement measures to strengthen the advantageous landscape features of green spaces. However, under the pressure of urbanization, only a limited quantity of land is left for expanding green spaces. Our results show that green space has decreased by a quarter in the Wuhan central city over the last two decades. Therefore, enhancing landscape patterns of green space deserves more attention. In terms of PM_{2.5} concentration, preserving larger natural patches and new increments around the existing green area are promising supplementary measures for locations with a lower proportion of green space and higher pollution emissions. These findings may serve as a reference for cities undergoing land-use conflicts and experiencing air pollution.

Author Contributions: Y.C.: data curation, methodology, writing—original draft preparation. X.K.: conceptualization, funding acquisition, supervision. M.M.: investigation, writing—review and editing. Y.Z. and Y.D.: software, visualization. L.T.: manuscript review. All of the authors contributed to improving the quality of the manuscript. X.K. is responsible for the academic opinion of this manuscript. All authors have read and agreed to the published version of the manuscript.

Funding: This study was funded by the National Natural Science Foundation of China (grant number 41971240), National Social Science later stage Foundation of China (grant number 19FGLB071), and The Ministry of Education of Humanities and Social Science project (grant number 18JHQ081).

Institutional Review Board Statement: Not applicable.

Informed Consent Statement: Not applicable.

Data Availability Statement: Not applicable.

Acknowledgments: The authors sincerely thank the anonymous reviewers for their insightful comments and suggestions. We also gratefully acknowledge the financial support from China Scholarship Council.

Conflicts of Interest: The authors declare no conflict of interest.

Appendix A

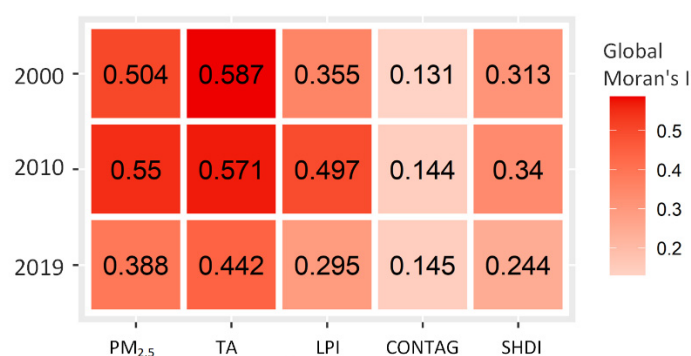


Figure A1. Global Moran's I of PM_{2.5} and green space landscape indexes (all of the Moran's I values are significant at the level of 1%).

Table A1. Examples of PM_{2.5} concentration guidelines.

Organizations/ Commissions/ Countries	Guidelines for PM _{2.5} (µg/m ³ , Annual Average)	Explanations	Reference	
WHO	Interim target 1	35	The Air quality guidelines (AQG) level was based on the relationship between PM _{2.5} and non-accidental mortality in the long run. The interim targets, as incremental steps, guide progressive air quality improvement for areas with high pollution.	[17]
	Interim target 2	25		
	Interim target 3	15		
	Interim target 4	10		
	AQG level	5		
European Commissions	Target value to be met as of 1.1.2010;	25	For a target value, countries are responsible to implement measures to ensure that it is attained. Limit value relates to the maximum margin of tolerance. Stage 2 is stricter than the former standards.	[20]
	Limit value to be met as of 1.1.2015			
	Stage 2 limit value to be met as of 1.1.2020			
China	Level 1	15	PM _{2.5} of natural reserve area and other protected places meet the Level 1; Residential area, factories, and rural area meet Level 2. No specific time limitation.	[18]
	Level 2	35		
India	National Ambient Air Quality Standard (NAAQS)	40	National standard released in 2009	[19]

References

- Feltynowski, M.; Kronenberg, J.; Bergier, T.; Kabisch, N.; Łaskiewicz, E.; Strohbach, M.W. Challenges of urban green space management in the face of using inadequate data. *Urban For. Urban Green.* **2018**, *31*, 56–66. [\[CrossRef\]](#)
- Stessens, P.; Canters, F.; Huysmans, M.; Khan, A.Z. Urban green space qualities: An integrated approach towards GIS-based assessment reflecting user perception. *Land Use Policy* **2020**, *91*, 104319. [\[CrossRef\]](#)

3. Berdejo-Espinola, V.; Suárez-Castro, A.F.; Amano, T.; Fielding, K.S.; Ying Oh, R.R.; Fuller, R.A. Urban green space use during a time of stress: A case study during the COVID-19 pandemic in Brisbane, Australia. *People Nat.* **2021**, *3*, 597–609. [[CrossRef](#)] [[PubMed](#)]
4. Matos, P.; Vieira, J.; Rocha, B.; Branquinho, C.; Pinho, P. Modeling the provision of air-quality regulation ecosystem service provided by urban green spaces using lichens as ecological indicators. *Sci. Total Environ.* **2019**, *665*, 521–530. [[CrossRef](#)] [[PubMed](#)]
5. Yao, L.; Li, T.; Xu, M.; Xu, Y. How the landscape features of urban green space impact seasonal land surface temperatures at a city-block-scale: An urban heat island study in Beijing, China. *Urban For. Urban Green.* **2020**, *52*, 126704. [[CrossRef](#)]
6. Ghosh, S.; Das, A. Modelling urban cooling island impact of green space and water bodies on surface urban heat island in a continuously developing urban area. *Model. Earth Syst. Environ.* **2018**, *4*, 501–515. [[CrossRef](#)]
7. Lindén, L.; Riikonen, A.; Setälä, H.; Yli-Pelkonen, V. Quantifying carbon stocks in urban parks under cold climate conditions. *Urban For. Urban Green.* **2020**, *49*, 126633. [[CrossRef](#)]
8. Venter, Z.S.; Barton, D.N.; Gundersen, V.; Figari, H.; Nowell, M.S. Back to nature: Norwegians sustain increased recreational use of urban green space months after the COVID-19 outbreak. *Landsc. Urban Plan.* **2021**, *214*, 104175. [[CrossRef](#)]
9. Partridge, D.R.; Clark, J.A. Urban green roofs provide habitat for migrating and breeding birds and their arthropod prey. *PLoS ONE* **2018**, *13*, 1–23. [[CrossRef](#)]
10. Ali-Taleshi, M.S.; Moeinaddini, M.; Riyahi Bakhtiari, A.; Feiznia, S.; Squizzato, S.; Bourliva, A. A one-year monitoring of spatiotemporal variations of PM_{2.5}-bound PAHs in Tehran, Iran: Source apportionment, local and regional sources origins and source-specific cancer risk assessment. *Environ. Pollut.* **2021**, *274*, 115883. [[CrossRef](#)]
11. Yang, D.; Wang, X.; Xu, J.; Xu, C.; Lu, D.; Ye, C.; Wang, Z.; Bai, L. Quantifying the influence of natural and socioeconomic factors and their interactive impact on PM_{2.5} pollution in China. *Environ. Pollut.* **2018**, *241*, 475–483. [[CrossRef](#)] [[PubMed](#)]
12. Dabass, A.; Talbott, E.O.; Rager, J.R.; Marsh, G.M.; Venkat, A.; Holguin, F.; Sharmae, R.K. Systemic inflammatory markers associated with cardiovascular disease and acute and chronic exposure to fine particulate matter air pollution (PM_{2.5}) among US NHANES adults with metabolic syndrome. *Environ. Res.* **2018**, *161*, 485–491. [[CrossRef](#)] [[PubMed](#)]
13. Lee, E.Y.; Oh, S.S.; White, M.J.; Eng, C.S.; Elhawary, J.R.; Borrell, L.N.; Nuckton, T.J.; Zeiger, A.M.; Keys, K.L.; Mak, A.C.Y.; et al. Ambient air pollution, asthma drug response, and telomere length in African American youth. *J. Allergy Clin. Immunol.* **2019**, *144*, 839–845.e10. [[CrossRef](#)] [[PubMed](#)]
14. Pierangeli, I.; Nieuwenhuijsen, M.J.; Cirach, M.; Rojas-Rueda, D. Health equity and burden of childhood asthma-related to air pollution in Barcelona. *Environ. Res.* **2020**, *186*, 109067. [[CrossRef](#)]
15. Geng, G.; Zheng, Y.; Zhang, Q.; Xue, T.; Zhao, H.; Tong, D.; Zheng, B.; Li, M.; Liu, F.; Hong, C.; et al. Drivers of PM_{2.5} air pollution deaths in China 2002–2017. *Nat. Geosci.* **2021**, *14*, 645–650. [[CrossRef](#)]
16. Li, X.; Zhang, T.; Sun, F.; Song, X.; Zhang, Y.; Huang, F.; Yuan, C.; Zhang, G.; Qi, F.; Shao, F. The relationship between particulate matter retention capacity and leaf surface micromorphology of ten tree species in Hangzhou, China. *Sci. Total Environ.* **2021**, *771*, 144812. [[CrossRef](#)]
17. WHO. Global Air Quality Guidelines: Particulate Matter (PM_{2.5} and PM₁₀), Ozone, Nitrogen Dioxide, Sulfur Dioxide and Carbon Monoxide. 2021. Available online: <https://www.who.int/publications/i/item/9789240034228> (accessed on 22 March 2022).
18. Ministry of Ecology and Environment of the People’s Republic of China. 2016. Ambient Air Quality Standards (GB 3095-2012). Available online: <https://www.mee.gov.cn/ywgz/fgbz/bz/bzwb/dqjhjhb/dqjhjzlbz/201203/W020120410330232398521.pdf> (accessed on 22 March 2022).
19. Chowdhury, S.; Dey, S.; Guttikunda, S.; Pillarisetti, A.; Smith, K.R.; Di Girolamo, L. Indian annual ambient air quality standard is achievable by completely mitigating emissions from household sources. *Proc. Natl. Acad. Sci. USA* **2019**, *116*, 10711–10716. [[CrossRef](#)]
20. European Commission. Air Quality Standards (Directive 2008/50/EU). 2008. Available online: <https://ec.europa.eu/environment/air/quality/standards.htm?msckid=1bed3d95cea811eca04359b8bb2ccff3> (accessed on 8 May 2022).
21. Ebenstein, A.; Fan, M.; Greenstone, M.; He, G.; Zhou, M. New evidence on the impact of sustained exposure to air pollution on life expectancy from China’s Huai River Policy. *Proc. Natl. Acad. Sci. USA* **2017**, *114*, 10384–10389. [[CrossRef](#)]
22. Apte, J.S.; Brauer, M.; Cohen, A.J.; Ezzati, M.; Pope, C.A. III. Ambient PM_{2.5} Reduces Global and Regional Life Expectancy. *Environ. Sci. Technol. Lett.* **2018**, *5*, 546–551. [[CrossRef](#)]
23. McGuinn, L.A.; Schneider, A.; McGarrah, R.W.; Ward-Caviness, C.; Neas, L.M.; Di, Q.; Schwartz, J.; Hauser, E.R.; Kraus, W.E.; Cascio, W.E.; et al. Association of long-term PM_{2.5} exposure with traditional and novel lipid measures related to cardiovascular disease risk. *Environ. Int.* **2019**, *122*, 193–200. [[CrossRef](#)]
24. Zhang, S.; Routledge, M.N. The contribution of PM_{2.5} to cardiovascular disease in China. *Environ. Sci. Pollut. Res.* **2020**, *27*, 37502–37513. [[CrossRef](#)]
25. Sandujav, C.; Ferreira, S.; Filipski, M.; Hashida, Y. Air pollution and happiness: Evidence from the coldest capital in the world. *Ecol. Econ.* **2021**, *187*, 107085. [[CrossRef](#)]
26. Zhao, N.; Liu, Y.; Vanos, J.K.; Cao, G. Day-of-week and seasonal patterns of PM_{2.5} concentrations over the United States: Time-series analyses using the Prophet procedure. *Atmos. Environ.* **2018**, *192*, 116–127. [[CrossRef](#)]
27. Zhao, X.; Zhou, W.; Han, L.; Locke, D. Spatiotemporal variation in PM_{2.5} concentrations and their relationship with socioeconomic factors in China’s major cities. *Environ. Int.* **2019**, *133*, 105145. [[CrossRef](#)] [[PubMed](#)]

28. Tapia, V.; Steenland, K.; Sarnat, S.E.; Vu, B.; Liu, Y.; Sánchez-Ccoylo, O.; Vasquez, V.; Gonzales, G.F. Time-series analysis of ambient PM_{2.5} and cardiorespiratory emergency room visits in Lima, Peru during 2010–2016. *J. Expo. Sci. Environ. Epidemiol.* **2020**, *30*, 680–688. [[CrossRef](#)] [[PubMed](#)]
29. Hammer, M.S.; van Donkelaar, A.; Li, C.; Lyapustin, A.; Sayer, A.M.; Hsu, N.C.; Levy, R.C.; Garay, M.J.; Kalashnikova, O.V.; Kahn, R.A.; et al. Global Estimates and Long-Term Trends of Fine Particulate Matter Concentrations (1998–2018). *Environ. Sci. Technol.* **2020**, *54*, 7879–7890. [[CrossRef](#)] [[PubMed](#)]
30. van Donkelaar, A.; Martin, R.V.; Li, C.; Burnett, R.T. Regional Estimates of Chemical Composition of Fine Particulate Matter Using a Combined Geoscience–Statistical Method with Information from Satellites, Models, and Monitors. *Environ. Sci. Technol.* **2019**, *53*, 2595–2611. [[CrossRef](#)]
31. Rastogi, N.; Singh, A.; Singh, D.; Sarin, M.M. Chemical characteristics of PM_{2.5} at a source region of biomass burning emissions: Evidence for secondary aerosol formation. *Environ. Pollut.* **2014**, *184*, 563–569. [[CrossRef](#)]
32. Roberts, G.; Wooster, M.J. Global impact of landscape fire emissions on surface level PM_{2.5} concentrations, air quality exposure and population mortality. *Atmos. Environ.* **2021**, *252*, 118210. [[CrossRef](#)]
33. Xu, G.; Ren, X.; Xiong, K.; Li, L.; Bi, X.; Wu, Q. Analysis of the driving factors of PM_{2.5} concentration in the air: A case study of the Yangtze River Delta, China. *Ecol. Indic.* **2020**, *110*, 105889. [[CrossRef](#)]
34. Zhang, X.; Gu, X.; Cheng, C.; Yang, D. Spatiotemporal heterogeneity of PM_{2.5} and its relationship with urbanization in North China from 2000 to 2017. *Sci. Total Environ.* **2020**, *744*, 140925. [[CrossRef](#)] [[PubMed](#)]
35. Yuan, M.; Yan, M.; Shan, Z. Is compact urban form good for air quality? A case study from china based on hourly smartphone data. *Land* **2021**, *10*, 504. [[CrossRef](#)]
36. Goyal, P.; Gulia, S.; Goyal, S.K. Review of land use specific source contributions in PM_{2.5} concentration in urban areas in India. *Air Qual. Atmos. Health* **2021**, *14*, 691–704. [[CrossRef](#)]
37. Xu, Z.; Niu, L.; Zhang, Z.; Hu, Q.; Zhang, D.; Huang, J.; Li, C. The impacts of land supply on PM_{2.5} concentration: Evidence from 292 cities in China from 2009 to 2017. *J. Clean. Prod.* **2022**, *347*, 131251. [[CrossRef](#)]
38. Han, L.; Zhao, J.; Gao, Y.; Gu, Z.; Xin, K.; Zhang, J. Spatial distribution characteristics of PM_{2.5} and PM₁₀ in Xi’an City predicted by land use regression models. *Sustain. Cities Soc.* **2020**, *61*, 102329. [[CrossRef](#)]
39. Liu, H.; Fang, C.; Zhang, X.; Wang, Z.; Bao, C.; Li, F. The effect of natural and anthropogenic factors on haze pollution in Chinese cities: A spatial econometrics approach. *J. Clean. Prod.* **2017**, *165*, 323–333. [[CrossRef](#)]
40. Beckerman, B.S.; Jerrett, M.; Serre, M.; Martin, R.V.; Lee, S.J.; van Donkelaar, A.; Ross, Z.; Su, J.; Burnett, R.T. A Hybrid Approach to Estimating National Scale Spatiotemporal Variability of PM_{2.5} in the Contiguous United States. *Environ. Sci. Technol.* **2013**, *47*, 7233–7241. [[CrossRef](#)]
41. Nowak, D.J.; Hirabayashi, S.; Bodine, A.; Hoehn, R. Modeled PM_{2.5} removal by trees in ten U.S. cities and associated health effects. *Environ. Pollut.* **2013**, *178*, 395–402. [[CrossRef](#)]
42. Wu, J.; Luo, K.; Wang, Y.; Wang, Z. Urban road greenbelt configuration: The perspective of PM_{2.5} removal and air quality regulation. *Environ. Int.* **2021**, *157*, 106786. [[CrossRef](#)]
43. Kim, K.; Jeon, J.; Jung, H.; Kim, T.K.; Hong, J.; Jeon, G.S.; Kim, H.S. PM_{2.5} reduction capacities and their relation to morphological and physiological traits in 13 landscaping tree species. *Urban For. Urban Green.* **2022**, *70*, 127526. [[CrossRef](#)]
44. Chen, M.; Dai, F.; Yang, B.; Zhu, S. Effects of urban green space morphological pattern on variation of PM_{2.5} concentration in the neighborhoods of five Chinese megacities. *Build. Environ.* **2019**, *158*, 1–15. [[CrossRef](#)]
45. Zhang, P.; Yang, L.; Ma, W.; Wang, N.; Wen, F.; Liu, Q. Spatiotemporal estimation of the PM_{2.5} concentration and human health risks combining the three-dimensional landscape pattern index and machine learning methods to optimize land use regression modeling in Shaanxi, China. *Environ. Res.* **2022**, *208*, 112759. [[CrossRef](#)] [[PubMed](#)]
46. Wu, H.T.; Yang, C.; Chen, J.; Yang, S.; Lu, T.; Lin, X. Effects of Green space landscape patterns on particulate matter in Zhejiang Province, China. *Atmos. Pollut. Res.* **2018**, *9*, 923–933. [[CrossRef](#)]
47. Ren, Y.; Qu, Z.; Du, Y.; Xu, R.; Ma, D.; Yang, G.; Shi, Y.; Fan, X.; Tani, A.; Guo, P.; et al. Air quality and health effects of biogenic volatile organic compounds emissions from urban green spaces and the mitigation strategies. *Environ. Pollut.* **2017**, *230*, 849–861. [[CrossRef](#)]
48. Churkina, G.; Kuik, F.; Bonn, B.; Lauer, A.; Grote, R.; Tomiak, K.; Butler, T.M. Effect of VOC Emissions from Vegetation on Air Quality in Berlin during a Heatwave. *Environ. Sci. Technol.* **2017**, *51*, 6120–6130. [[CrossRef](#)]
49. Berglihn, E.C.; Gómez-Baggethun, E. Ecosystem services from urban forests: The case of Osloomarka, Norway. *Ecosyst. Serv.* **2021**, *51*, 101358. [[CrossRef](#)]
50. Wei, J.; Li, Z.; Lyapustin, A.; Sun, L.; Peng, Y.; Xue, W.; Su, T.; Cribb, M. Reconstructing 1-km-resolution high-quality PM_{2.5} data records from 2000 to 2018 in China: Spatiotemporal variations and policy implications. *Remote Sens. Environ.* **2021**, *252*, 112136. [[CrossRef](#)]
51. Wuhan Municipal Statistics Bureau. Wuhan Statistical Yearbook (2021). China Statistics Press. Available online: http://tjj.wuhan.gov.cn/tjfw/tjnj/202112/t20211220_1877108.shtml (accessed on 22 March 2022). (In Chinese)
52. Central Government of the People’s Republic of China. China’s 14th Five-Year Plan (2021–2025). 2021. Available online: http://www.gov.cn/xinwen/2021-03/13/content_5592681.htm (accessed on 8 May 2022). (In Chinese)

53. General Administration of Quality Supervision, Inspection and Quarantine of the People's Republic of China, Standardization Administration of China. Current Land Use Classification in China (GB/T 21010-2017). 2017. Available online: <http://openstd.samr.gov.cn/bzgk/gb/newGbInfo?hcno=224BF9DA69F053DA22AC758AAAADFEAA&msclid=4a83d0c8ceb611ec9e7d88f816f28a40> (accessed on 8 May 2022). (In Chinese)
54. Google Earth. Available online: <https://www.google.de/intl/de/earth> (accessed on 8 May 2022).
55. GlobalLand30. Available online: <http://www.globallandcover.com/> (accessed on 20 March 2022).
56. ChinaHighPM2.5 dataset. Available online: <https://weijing-rs.github.io/product.html> (accessed on 13 March 2022).
57. Data Center of Resources and Environmental Sciences. Available online: <https://www.resdc.cn/> (accessed on 13 March 2022).
58. Huang, B.X.; Chiou, S.C.; Li, W.Y. Landscape Pattern and Ecological Network Structure in Urban Green Space Planning: A Case Study of Fuzhou City. *Land* **2021**, *10*, 769. [[CrossRef](#)]
59. Zambrano, L.; Handel, S.N.; Fernandez, T.; Brostella, I. Landscape spatial patterns in Mexico City and New York City: Contrasting territories for biodiversity planning. *Landsc. Ecol.* **2022**, *37*, 601–617. [[CrossRef](#)]
60. Madanian, M.; Soffianian, A.R.; Koupai, S.S.; Pourmanafi, S.; Momeni, M. Analyzing the effects of urban expansion on land surface temperature patterns by landscape metrics: A case study of Isfahan city, Iran. *Environ. Monit. Assess.* **2018**, *190*, 189. [[CrossRef](#)]
61. Nastran, M.; Kobal, M.; Eler, K. Urban heat islands in relation to green land use in European cities. *Urban For. Urban Green.* **2019**, *37*, 33–41. [[CrossRef](#)]
62. Ritters, K.H.; O'Neill, R.V.; Wickham, J.D. A note on contagion indices for landscape analysis. *Landsc. Ecol.* **1996**, *11*, 197–202. [[CrossRef](#)]
63. Grafius, D.R.; Corstanje, R.; Harris, J.A. Linking ecosystem services, urban form and green space configuration using multivariate landscape metric analysis. *Landsc. Ecol.* **2018**, *33*, 557–573. [[CrossRef](#)] [[PubMed](#)]
64. Karimi, J.D.; Corstanje, R.; Harris, J.A. Understanding the importance of landscape configuration on ecosystem service bundles at a high resolution in urban landscapes in the UK. *Landsc. Ecol.* **2021**, *36*, 2007–2024. [[CrossRef](#)]
65. Mears, M.; Brindley, P.; Jorgensen, A.; Ersoy, E.; Maheswaran, R. Greenspace spatial characteristics and human health in an urban environment: An epidemiological study using landscape metrics in Sheffield, UK. *Ecol. Indic.* **2019**, *106*, 105464. [[CrossRef](#)]
66. Guan, Y.; Li, X.; Li, S.; Sun, H.; Liu, H. Effect of Urban fringes green space fragmentation on ecosystem service value. *PLoS ONE* **2022**, *17*, 1–16. [[CrossRef](#)] [[PubMed](#)]
67. Anselin, L. Local indicators of spatial association—LISA. *Geogr. Anal.* **1995**, *27*, 93–115. [[CrossRef](#)]
68. Jesri, N.; Saghaipour, A.; Koochpai, A.; Farzinnia, B.; Jooshin, M.K.; Abolkheirian, S.; Sarvi, M. Mapping and Spatial Pattern Analysis of COVID-19 in Central Iran Using the Local Indicators of Spatial Association (LISA). *BMC Public Health* **2021**, *21*, 2227. [[CrossRef](#)]
69. Geary, R. The Contiguity Ratio and Statistical Mapping. *Inc. Stat.* **1954**, *5*, 115–146. [[CrossRef](#)]
70. Anselin, L. A local indicator of multivariate spatial association: Extending Geary's c. *Geogr. Anal.* **2019**, *51*, 133–150. [[CrossRef](#)]
71. Golgher, A.B.; Voss, P.R. How to Interpret the Coefficients of Spatial Models: Spillovers, Direct and Indirect Effects. *Spat. Demogr.* **2016**, *4*, 175–205. [[CrossRef](#)]
72. Lee, L.; Yu, J. Estimation of spatial autoregressive panel data models with fixed effects. *J. Econom.* **2010**, *154*, 165–185. [[CrossRef](#)]
73. Anselin, L. *Exploring Spatial Data with GeoDaTM: A Workbook*; Center for Spatially Integrated Social Science: Fairfax, VA, USA, 2005; pp. 165–223.
74. Chen, Y.; Shao, S.; Fan, M.; Tian, Z.; Yang, L. One man's loss is another's gain: Does clean energy development reduce CO₂ emissions in China? Evidence based on the spatial Durbin model. *Energy Econ.* **2022**, *107*, 105852. [[CrossRef](#)]
75. LeSage, J.; Pace, R.K. *Introduction to Spatial Econometrics*, 1st ed.; Chapman and Hall/CRC: New York, NY, USA, 2009. [[CrossRef](#)]
76. Kuha, J. AIC and BIC: Comparisons of Assumptions and Performance. *Sociol. Methods Res.* **2004**, *33*, 188–229. [[CrossRef](#)]
77. Feng, R.; Wang, F.; Wang, K.; Xu, S. Quantifying influences of anthropogenic-natural factors on ecological land evolution in mega-urban agglomeration: A case study of Guangdong-Hong Kong-Macao greater Bay area. *J. Clean. Prod.* **2021**, *283*, 125304. [[CrossRef](#)]
78. Wang, Z.; Li, C.; Yang, T. Spatial–Temporal Variations of Green Space in Metropolitan Area: The Case of Wuhan, China. In *Human-Centered Urban Planning and Design in China: Volume I*; Li, W., Hu, L., Cao, J., Eds.; Geo Journal Library; Springer: Cham, Switzerland, 2021; Volume 129. [[CrossRef](#)]
79. Zhang, Q.; Zheng, Y.; Tong, D.; Shao, M.; Wang, S.; Zhang, Y.; Xue, X.; Wang, J.; He, H.; Liu, W.; et al. Drivers of improved PM_{2.5} air quality in China from 2013 to 2017. *Proc. Natl. Acad. Sci. USA* **2019**, *116*, 24463–24469. [[CrossRef](#)]
80. Wuhan Municipal Bureau of Ecology and Environment. Wuhan Urban Ambient Air Quality Compliance Plan (2013–2027). 8 October 2014. Available online: http://hbj.wuhan.gov.cn/fbjd_19/xxgkml/gjhj/lsgj/202004/t20200427_1143153.html (accessed on 11 May 2022). (In Chinese)
81. Stern, D.I.; Common, M.S.; Barbier, E.B. Economic growth and environmental degradation: The environmental Kuznets curve and sustainable development. *World Dev.* **1996**, *24*, 1151–1160. [[CrossRef](#)]
82. Cheng, Z.; Li, L.; Liu, J. Identifying the spatial effects and driving factors of urban PM_{2.5} pollution in China. *Ecol. Indic.* **2017**, *82*, 61–75. [[CrossRef](#)]

83. Zhou, T.; Hu, H.; Chen, J.; Bai, R.; Wang, F.; Wang, Y.; Zhang, J.; Liu, X.; Chen, N.; Xu, K. Analysis on the contribution rates of point and area source emissions to Wuhan SO₂, NO₂, PM_{2.5} concentrations and atmospheric environmental capacity. *Atmos. Pollut. Res.* **2021**, *12*, 101209. [[CrossRef](#)]
84. Wang, H.; Li, J.; Peng, Y.; Zhang, M.; Che, H.; Zhang, X. The impacts of the meteorology features on PM_{2.5} levels during a severe haze episode in central-east China. *Atmos. Environ.* **2019**, *197*, 177–189. [[CrossRef](#)]
85. Chen, J.; Zhu, L.; Fan, P.; Tian, L.; Laforteza, R. Do green spaces affect the spatiotemporal changes of PM_{2.5} in Nanjing? *Ecol. Process.* **2016**, *5*, 1–13. [[CrossRef](#)] [[PubMed](#)]
86. Yu, M.; Zhou, W.; Zhao, X.; Liang, X.; Wang, Y.; Tang, G. Is Urban Greening an Effective Solution to Enhance Environmental Comfort and Improve Air Quality? *Environ. Sci. Technol.* **2022**, *56*, 5390–5397. [[CrossRef](#)] [[PubMed](#)]
87. Donato, A.; Conte, M.; Grasso, F.M.; Contini, D. Seasonal and diurnal behaviour of size segregated particles fluxes in a suburban area. *Atmos. Environ.* **2019**, *219*, 117052. [[CrossRef](#)]
88. Xing, Y.; Brimblecombe, P. Role of vegetation in deposition and dispersion of air pollution in urban parks. *Atmos. Environ.* **2019**, *201*, 73–83. [[CrossRef](#)]
89. Lu, S.; Yang, X.; Li, S.; Chen, B.; Jiang, Y.; Wang, D.; Xu, L. Effects of plant leaf surface and different pollution levels on PM_{2.5} adsorption capacity. *Urban For. Urban Green.* **2018**, *34*, 64–70. [[CrossRef](#)]
90. Jayasooriya, V.M.; Ng, A.W.M.; Muthukumaran, S.; Perera, B.J.C. Green infrastructure practices for improvement of urban air quality. *Urban For. Urban Green.* **2017**, *21*, 34–47. [[CrossRef](#)]
91. Vieira, J.; Matos, P.; Mexia, T.; Silva, P.; Lopes, N.; Freitas, C.; Correia, O.; Santos-Reis, M.; Branquinho, C.; Pinho, P. Green spaces are not all the same for the provision of air purification and climate 514 regulation services: The case of urban parks. *Environ. Res.* **2018**, *160*, 306–313. [[CrossRef](#)]
92. Jaafari, S.; Shabani, A.A.; Moeinaddini, M.; Daneshkar, A.; Sakieh, Y. Applying landscape metrics and structural equation modeling to predict the effect of urban green space on air pollution and respiratory mortality in Tehran. *Environ. Monit. Assess.* **2020**, *192*, 412. [[CrossRef](#)]
93. Zheng, H.; Kong, S.; Chen, N.; Yan, Y.; Liu, D.; Zhu, B.; Xu, K.; Cao, W.; Ding, Q.; Lan, B. Significant changes in the chemical compositions and sources of PM_{2.5} in Wuhan since the city lockdown as COVID-19. *Sci. Total Environ.* **2020**, *739*, 140000. [[CrossRef](#)]
94. Singh, R.P.; Chauhan, A. Impact of lockdown on air quality in India during COVID-19 pandemic. *Air Qual. Atmos. Health* **2020**, *13*, 921–928. [[CrossRef](#)]
95. Balasubramaniam, D.; Kanmanipappa, C.; Shankarlal, B.; Saravanan, M. Assessing the impact of lockdown in US, Italy and France—What are the changes in air quality? *Energy Sources Part A Recover. Util. Environ. Eff.* **2020**, 1–11. [[CrossRef](#)]
96. Dinoi, A.; Gulli, D.; Ammoscato, I.; Calidonna, C.R.; Contini, D. Impact of the Coronavirus Pandemic Lockdown on Atmospheric Nanoparticle Concentrations in Two Sites of Southern Italy. *Atmosphere* **2021**, *12*, 352. [[CrossRef](#)]
97. Jephcote, C.; Hansell, A.L.; Adams, K.; Gulliver, J. Changes in air quality during COVID-19' lockdown' in the United Kingdom. *Environ. Pollut.* **2021**, *272*, 116011. [[CrossRef](#)]
98. Tobías, A.; Carnerero, C.; Reche, C.; Massagué, J.; Via, M.; Minguillón, M.C.; Alastuey, A.; Querol, X. Changes in air quality during the lockdown in Barcelona (Spain) one month into the SARS-CoV-2 epidemic. *Sci. Total Environ.* **2020**, *726*, 138540. [[CrossRef](#)] [[PubMed](#)]
99. Zhao, X.; Cheng, Z.; Jiang, C. Could air quality get better during epidemic prevention and control in China? An analysis based on regression discontinuity design. *Land* **2021**, *10*, 373. [[CrossRef](#)]
100. Kumari, P.; Toshniwal, D. Impact of lockdown on air quality over major cities across the globe during COVID-19 pandemic. *Urban Clim.* **2020**, *34*, 100719. [[CrossRef](#)]
101. Lian, X.; Huang, J.; Huang, R.; Liu, C.; Wang, L.; Zhang, T. Impact of city lockdown on the air quality of COVID-19-hit of Wuhan city. *Sci. Total Environ.* **2020**, *742*, 140556. [[CrossRef](#)]